J Electr Eng Technol.2018; 13(1): 287-297
http://doi.org/10.5370/JEET.2018.13.1.287

ISSN(Print) 1975-0102
ISSN(Online) 2093-7423

A Novel Speed Estimation Method of Induction Motors Using Real-Time Adaptive Extended Kalman Filter

Yanqing Zhang*, Zhonggang Yin†, Guoyin Li, Jing Liu*** and Xiangqian Tong***

Abstract – To improve the performance of sensorless induction motor (IM) drives, a novel speed estimation method based on the real-time adaptive extended Kalman filter (RAEKF) is proposed in this paper. In this algorithm, the fuzzy factor is introduced to tune the measurement covariance matrix online by the degree of mismatch between the actual innovation and the theoretical. Simultaneously, the fuzzy factor can be continuously self-tuned tuned by the fuzzy logic reasoning system based on Takagi–Sugeno (T-S) model. Therefore, the proposed method improves the model adaptability to the actual systems and the environmental variations, and reduces the speed estimation error. Furthermore, a simple exponential function based on the fuzzy theory is used to reduce the computational burden, and the real-time performance of the system is improved. The correctness and the effectiveness of the proposed method are verified by the simulation and experimental results.

Keywords: Induction motor (IM), Speed estimation, Real-time adaptive extended Kalman filter (RAEKF), Fuzzy factor

1. Introduction

In the AC drive systems of high performance, the closed-loop speed control is indispensable. Generally, the speed is measured by speed sensors. However, the cost is increased, and the robustness and the reliability of system are reduced owing to installation of speed sensors. These problems make scholars have done a lot of researches on the speed sensorless control. Many sensorless methods have been proposed, such as artificial neural networks (ANN) [1], model reference adaptive systems (MRAS) [2, 3], sliding-mode observer (SMO) [4, 5], adaptive full-order observer (AFO) [6-8], high-frequency signal injection [9, 10], and extended Kalman filter (EKF) [11-26].

Sun *et al*. [1] propose a novel method which uses ANNs for the parameter estimation for IM to implement sensorless control, and the performance of proposed method is better than classical one. Accetta *et al*. [2] have developed a speed observer based on a closed-loop MRAS for linear induction motor drives, and the low speed performance is improved based on this method. Orlowska-Kowalska and Dybkowski. [3] propose a novel formulation of reactive-power-based MRAS, which can operate stably in the four quadrants. However, in this research, with respect to sensorless IM drives, the rotor flux and the load torque should be known to achieve the sensorless controller. In addition, the effectiveness is lost, and the accurate results are not obtained due to the unobservability at low speed in these observers. References [4] and [5] use SMO for speed estimation and stator resistance identification, and thus the problems of stator resistance variation are overcome, particularly at low speed operation. However, since the method relies on the mathematical model of IM in the design process, and the observation ability is commonly lost at zero frequency. In addition, the problem of SMO which is chatter should be solved. In [6, 7] and [8], some novel designing rules for the self-adaption of PI gains to obtain satisfied performances are proposed. The robustness of AFO against motor parameter variations is also researched, but the speed fluctuation becomes larger with the speed decreased. In [9, 10], the high-frequency signal injection is used for rotor speed estimation, and good performance is obtained. The speed-sensorless control approaches using signal injection can remain stable for a long time at zero stator frequency. However, they are highly complicated and need customized designs for specific motor drive, and the estimated speed is delayed to the totor speed due to the filters.

Compared with the other methods, a stochastic method is used for state estimation in EKF, and differential operation of estimated state is avoided. The estimated value can be adjusted by gain matrix and innovation error, which makes state estimation error tend to be minimum. EKF has become the focus of the speed sensorless control for motors. In [11], the convergence of EKF in sensorless drive system of induction motor is analyzed, and the related properties of discrete model are discussed. Moreover, the observable condition of EKF is researched deeply, and the properties and the estimator performance are verified by experimental results. Reference [12] uses EKF for speed

† Corresponding Author: Dept. of Electrical Engineering, Xi'an University of Technology, China. (zhgyin@xaut.edu.cn)
* Dept. of Electrical Engineering, Xi'an University of Technology, China. (zhangyanqing029@163.com, lstong@mail.xaut.edu.cn, jingliu@xaut.edu.cn)
** CRRC SRI Chongqing S&T Co., Ltd, China. (liguoyin199@163.com)
Received: May 29, 2017; Accepted: October 1, 2017

and flux linkage estimation in direct torque control (DTC) system, and the experimental results indicated that the system using EKF has satisfactory performance and practical value. In [13], EKF is used for speed, flux linkage, and stator current estimation in the induction motor predictive control, the estimated current is fed back into the prediction model to reduce the current harmonics. Based on this method, the good performance can be achieved in the wide speed range, including the field weakening region. In [14] and [15], a speed and position estimator based on EKF is used in the vector control system of PMSM. The proposed method enhances the control bandwidth and avoids the identification problems due to low order state equations of IPMSM, and the rotor position estimation error using the identified flux is limited to a small level. To improve the practicability of EKF, references [16] and [17] propose a reduced-order EKF algorithm to only estimate the flux and speed estimation, and the speed and flux linkage can be estimated easily. In order to reduce the influence of motor parameter variations, Barut *et al*. [18] propose a bi input-EKF (BI-EKF)-based estimator, the proposed method estimation is verified in real-time with the challenging variations of motor parameters in a wide speed range. Compared with EKF, the performance of BI-EKF has made significant improvement.

However, EKF requires good prior information about the measurement noise condition to achieve the superior estimated performance. The researches show that the system may lose stability in different noise conditions even EKF is accurate. The estimation performance of EKF will become worse due to large external disturbance and time varied measurement noise. Therefore, the noise covariance matrices selected by the prior information cause the bad performance of estimation, and the filter is also unsteady under different noise condition. The different measurement noise disturbance will degrade the performance of EKF with the fixed measurement covariance matrix. An adaptive speed and flux estimation method based on the multiple-model extended Kalman filter (MM-EKF) for induction motors is proposed in [19], and the experimental results demonstrate that MM-EKF can effectively improve the model adaptability to the actual systems and the environmental variations. Moreover, the maximum error of the speed estimation with disturbance and motor parameter mismatches is obviously reduced, and both the steady and transient performance is improved by using the proposed adaptive speed estimation method. However, the computation of algorithm is large, and the high performance for CPU is required. In [20], a speed estimation method based on strong tracking EKF with least-square for induction motors is proposed, and the good robustness and anti-error performance are obtained. However, the symmetry of error covariance matrix cannot be ensured based this method, which resulting in filtering divergence. The main contribution of this paper is that a novel speed estimation method based on the real-time adaptive extended Kalman filter (RAEKF) is proposed in this paper to improve the model adaptability to the actual systems and the environmental variations, and reduce the speed estimation error. In this algorithm, the fuzzy factor is introduced to tune the measurement covariance matrix online, and the estimation error is adjusted adaptively and the mutational state is tracked fast. Simultaneously, the fuzzy factor can be continuously self-tuned tuned by the fuzzy logic reasoning system based on Takagi-Sugeno (T-S) model. Furthermore, a simple exponential function based on the fuzzy theory is used to reduce the computational burden, and the real-time performance of the system is improved. The correctness and the effectiveness of the proposed method are verified by the simulation and experimental results.

2. EKF Observer

The state equations for IM is expressed as follows,

$$\frac{di_{s\alpha}}{dt} = (-\frac{R_s}{\sigma L_s} + \frac{1-\sigma}{\sigma T_r})i_{s\alpha} + \frac{L_m}{\sigma L_s L_r T_r}\psi_{r\alpha} + \omega_r \frac{L_m}{\sigma L_s L_r}\psi_{r\beta} + \frac{1}{\sigma L_s}u_{s\alpha} \tag{1}$$

$$\frac{di_{s\beta}}{dt} = (-\frac{R_s}{\sigma L_s} + \frac{1-\sigma}{\sigma T_r})i_{s\beta} - \omega_r \frac{L_m}{\sigma L_s L_r}\psi_{r\alpha} + \frac{L_m}{\sigma L_s L_r T_r}\psi_{r\beta} + \frac{1}{\sigma L_s}u_{s\beta} \tag{2}$$

$$\frac{d\psi_{r\alpha}}{dt} = \frac{L_m}{T_r}i_{s\alpha} - \frac{1}{T_r}\psi_{r\alpha} - \omega_r\psi_{r\beta} \tag{3}$$

$$\frac{d\psi_{r\beta}}{dt} = \frac{L_m}{T_r}i_{s\beta} - \frac{1}{T_r}\psi_{r\beta} + \omega_r\psi_{r\alpha} \tag{4}$$

$$\frac{d\omega_r}{dt} = \frac{p^2 L_m}{JL_r}(i_{s\beta}\psi_{r\alpha} - i_{s\alpha}\psi_{r\beta}) - \frac{p}{J}T_L \tag{5}$$

$$\boldsymbol{Y} = \left[i_{s\alpha} \ \ i_{s\beta} \right]^T \tag{6}$$

In the speed sensorless control, the models which are described by (1)-(6) are non-linear and multivariable, and is affected by parametric uncertainties. The change of speed can be ignored when the sampling period is very small or the load moment of inertia is very large. Therefore, a fifth-order model is obtained based on the assumption that $\dot{\omega}_r = 0$ without torque observation.

EKF can be described by

$$\frac{d\hat{x}}{dt} = A\hat{x} + Bu + K(y - \hat{y}) \tag{7}$$

$$\hat{y} = H\hat{x} \tag{8}$$

The noise exists in the actual system, which can be incorporated in vector w_k and vector v_k.

$$\mathrm{cov}(v_k, v_i) = E\{v_k v_i^T\} = \begin{cases} Q, i = k \\ 0, i \neq k \end{cases} \tag{9}$$

$$\mathrm{cov}(w_k, w_i) = E\{w_k w_i^T\} = \begin{cases} R, i = k \\ 0, i \neq k \end{cases} \tag{10}$$

$$\mathrm{cov}(v_k, w_i) = E\{v_k w_i^T\} = 0,\ \text{for all } i \text{ and } k \tag{11}$$

In the recursive calculation of EKF, w_k and v_k are not used directly, but Q and R are used. The system noise covariance Q includes model uncertain, motor parameter inaccuracy, system disturbances, and rounding and truncation error caused by limited word length of DSP. The noise covariance R includes A/D quantization and measurement noise introduced by the current sensors.

From (7) and (8), EKF is expressed by the following nonlinear model under taking noise into consideration in the α-β reference frame,

$$\hat{x}_k = A'\hat{x}_{k-1} + B'u_k + K_k(y - \hat{y}) \tag{12}$$

$$\hat{y}_k = H_k \hat{x}_k \tag{13}$$

$x_k = (i_{s\alpha,k}\ i_{s\beta,k}\ \psi_{r\alpha,k}\ \psi_{r\beta,k}\ \omega_{r,k})^T$, $u_k = (u_{s\alpha,k}\ u_{s\beta,k})^T$,

$$A_k = \begin{bmatrix} 1-\dfrac{T}{T'_{sr}} & 0 & \dfrac{TL_m}{\sigma L_s L_r T_r} & \hat{\omega}_r \dfrac{TL_m}{\sigma L_s L_r} & 0 \\ 0 & 1-\dfrac{T}{T'_{sr}} & -\hat{\omega}_r \dfrac{TL_m}{\sigma L_s L_r} & \dfrac{TL_m}{\sigma L_s L_r T_r} & 0 \\ \dfrac{TL_m}{T_r} & 0 & 1-\dfrac{T}{T_r} & -T\hat{\omega}_r & 0 \\ 0 & \dfrac{TL_m}{T_r} & T\hat{\omega}_r & 1-\dfrac{T}{T_r} & 0 \\ 0 & 0 & 0 & 0 & 1 \end{bmatrix}$$

$$B_k = \begin{bmatrix} \dfrac{T}{\sigma L_s} & 0 \\ 0 & \dfrac{T}{\sigma L_s} \\ 0 & 0 \\ 0 & 0 \\ 0 & 0 \end{bmatrix},\quad H_k = \begin{bmatrix} 1 & 0 & 0 & 0 & 0 \\ 0 & 1 & 0 & 0 & 0 \end{bmatrix}$$

$T'_{sr} = \dfrac{\sigma L_s}{R_{sr}}$, $T_r = \dfrac{L_r}{R_r}$, $R_{sr} = R_s + \dfrac{L_m^2}{L_r T_r}$.

Prediction Process:

$$\tilde{x}_k = A_k \hat{x}_{k-1} + B_k u_k \tag{14}$$

$$\tilde{P}_k = G_k \hat{P}_{k-1} G_k^T + Q_k \tag{15}$$

where $G_k = \dfrac{\partial}{\partial x}\left(A_k x + B_k u\right)\Big|_{x=\tilde{x}_k}$

$$= \begin{bmatrix} 1-\dfrac{T}{T'_{sr}} & 0 & \dfrac{TL_m}{\sigma L_s L_r T_r} & \tilde{\omega}_{r,k}\dfrac{TL_m}{\sigma L_s L_r} & \dfrac{TL_m}{\sigma L_s L_r}\tilde{\psi}_{r\beta,k} \\ 0 & -\dfrac{T}{T'_{sr}} & -\tilde{\omega}_{r,k}\dfrac{TL_m}{\sigma L_s L_r} & \dfrac{TL_m}{\sigma L_s L_r T_r} & -\dfrac{TL_m}{\sigma L_s L_r}\tilde{\psi}_{r\alpha,k} \\ \dfrac{TL_m}{T_r} & 0 & 1-\dfrac{T}{T_r} & -T\tilde{\omega}_{r,k} & -T\tilde{\psi}_{r\beta,k} \\ 0 & \dfrac{TL_m}{T_r} & T\tilde{\omega}_{r,k} & 1-\dfrac{T}{T_r} & T\tilde{\psi}_{r\alpha,k} \\ 0 & 0 & 0 & 0 & 1 \end{bmatrix}$$

Kalman Filter Gain:

$$K_k = \tilde{P}_k H_k^T (H_k \tilde{P}_k H_k^T + R_k)^{-1} \tag{16}$$

FilterProcess:

$$\hat{x}_k = \tilde{x}_k + K_k(y_k - H_k \tilde{x}_k) \tag{17}$$

$$\hat{P}_k = (I - K_k H_k)\tilde{P}_k \tag{18}$$

3. Real-Time Adaptive EKF Observer

In the traditional EKF, the noise covariance matrix is unitary so that it cannot adjust different situations and work modes. Moreover, extended Kalman filter is poorly robust against model uncertainties. When the motor running state does not conform to the model, there is a greater speed estimation error.

A novel speed estimation method based on the real-time adaptive extended Kalman filter (RAEKF) is proposed in this paper to improve the model adaptability to the actual systems and the environmental variations, and reduces the speed estimation error. In this algorithm, the fuzzy factor is introduced to tune the measurement covariance matrix online, and the estimation error is adjusted adaptively and the mutational state is tracked fast. Simultaneously, the fuzzy factor can be continuously self-tuned tuned by the fuzzy logic reasoning system based on Takagi–Sugeno (T-S) model. Furthermore, a simple exponential function based on the fuzzy theory is used to reduce the computational burden, and the real-time performance of the system is improved.

The innovation of filter is a parameter which can be observed directly, and it can be used as a reference for the filter performance by observing the covariance of the innovation sequence. Generally, the innovation of filter should be a white noise sequence with zero mean. However, the statistical characteristics of the innovation sequence will become complex, when the prior knowledge of the measurement noise is not known exactly. Therefore, through the innovation covariance estimation, the measurement noise covariance matrix R can be adjusted adaptively.

r_k is the innovation at k moment, it can be calculated as follows

$$r_k = y_k - H_k \tilde{x}_k \tag{19}$$

The actual innovation covariance can be computed through averaging within a sliding estimation window, and it can be obtained as follows

$$c_r = \frac{1}{M}\sum_{i=i_0}^{k} r_i r_i^T \tag{20}$$

where i_0 is the first sample inside the window, and $i_0=k-M+1$. The window size M is chosen empirically to make statistical smoothing. If the window size M is too small, the actual innovation covariance will be too noisy. On the other hand, if a large window size is utilized, the actual innovation covariance will be smoother.

Then, the theoretical innovation covariance of EKF with a fixed R should be

$$p_r = H_k(G_k P_{k\text{-}1} G_k^T + Q)H_k^T + R_k \tag{21}$$

When EKF is performed optimally, the actual innovation covariance should be approximately equal to the theoretical innovation covariance, namely ,

$$c_r \approx p_r \tag{22}$$

Obviously, the selection of measurement noise matrix R is important for the convergence of the speed estimation based on EKF. The influence of large disturbance can be reduced or eliminated by modulating measurement noise matrix on the basis of the innovation.

The structure of AEKF algorithm is presented as follows:

Prediction:

$$\tilde{x}_k = f(\hat{x}_{k-1}) \tag{23}$$

$$\tilde{P}_k = G_k \hat{P}_{k-1} G_k^T + Q_k \tag{24}$$

Update:

$$K_k = \tilde{P}_k H_k^T (H_k \tilde{P}_k H_k^T + R_k)^{-1} \tag{25}$$

$$\hat{x}_k = \tilde{x}_k + K_k(y_k - H_k \tilde{x}_k) \tag{29}$$

$$\hat{P}_k = \tilde{P}_k - K_k H_k \tilde{P} \tag{27}$$

$$R_{k+1} = s_{k+1}^b R_k \tag{28}$$

where s_k is an adaptive adjustment factor, which is used to adjust the measurement noise matrix R_k, and $b(b>0)$ is an amplification coefficient of the adaptive level.

The main difference between real-time adaptive EKF and EKF is the calculation of factor s_{k+1}^b. If $s_{k+1}^b = 1$, AEKF is the same as the traditional EKF.

If it is found that the actual value of the innovation covariance has discrepancy with its theoretical value, the diagonal elements of R_k is adjusted based on the size of this discrepancy. The objective of these adjustments is to correct this mismatch as far as possible. The ratio of trace between theoretic innovation and actual innovation can be defined as the degree of mismatch (DOM_k)

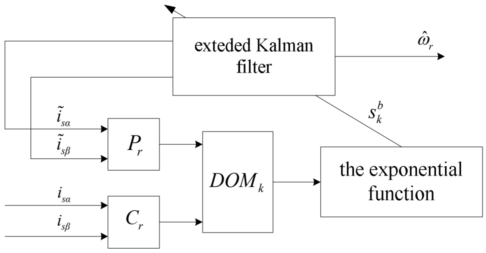

Fig. 1. Speed estimation structure based on AEKF

$$DOM_k = \frac{Tr(c_r)}{Tr(p_r)} \tag{29}$$

where $Tr(\cdot)$ is the trace of matrix. According to (22), when EKF is performed optimally, DOM_k should be around one. The block diagram of real-time adaptive EKF is shown in Fig. 1.

In AEKF, the degree of mismatch (DOM_k) parameter is monitored based on the innovation, and then the exponential function is designed to adjust the adjustment factor s_k dynamically for EKF under uncertain noise circumstances.

The amplification coefficient b is essential to the adaptive adjustment factor s_k for predicting the measurement noise matrix R_k in practical applications.

a) If $b>1$, it indicates that b magnifies effect of the adjustment of s_k. Therefore, R_k can be modified within less steps, and adjusted to optimum rapidly. However, if the selected b is too large, it may causes that the value of R_k fluctuates with a small amplitude.
b) If $b<1$, it indicates b minifies effect of the adjustment of s_k. Therefore, R_k can be adjusted to optimum precisely and stably. However, if the selected b is too small, it may need more transition time which is used to adjust R_k .

3.1 Seeking mechanism of adjustment factor based on fuzzy logic

The fuzzy logic is developed by Zadeh for representing uncertain and imprecise knowledge. It provides an approximate but effective method to describe the behavior of systems which are too complex, ill-defined, or not easily analyzed mathematically. In Fig. 2, a typical fuzzy system consists of three components: fuzzification, fuzzy reasoning (fuzzy inference), and fuzzy defuzzification.

As mentioned above, when the actual innovation covariance has extreme discrepancy with the theoretical innovation covariance, it shows that there are presumable variations in measurement noises. Therefore, the filter cannot reach the optimum performance based on the fixed

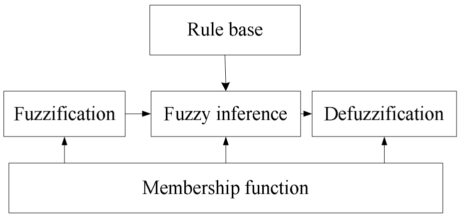

Fig. 2. A fuzzy system

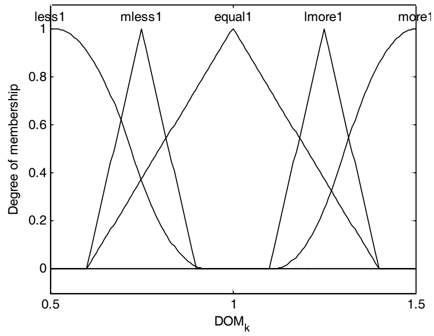

(a)

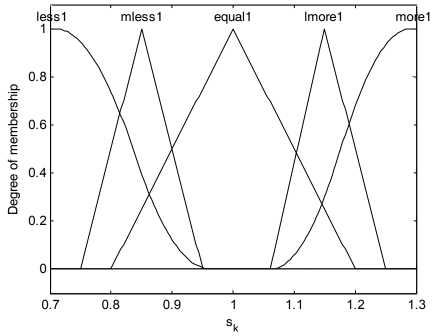

(b)

Fig. 3. Membership functions of input and output variable of FIS: (a) Membership functions of DOM_k; (b) Membership functions of s_k

measurement noise matrix R. In order to get optimized extended Kalman filter, the system selects an adaptive adjustment factor s_k from an appropriate fuzzy logic controller to make the actual value of the innovation covariance close to the theoretical value.

There are one input and one output for the fuzzy logic controller (FLC), and 5 rules are used, namely,

IF $DOM_k \in$ less1, then $s_k \in$ less1.
IF $DOM_k \in$ equal1, then $s_k \in$ equal1.
IF $DOM_k \in$ more1, then $s_k \in$ more1.
IF $DOM_k \in$ mless1, then $s_k \in$ mless1.
IF $DOM_k \in$ lmore1, then $s_k \in$ lmore1.

These membership functions are provided in Fig. 3.

The fuzzy modeling is a method to describe the characteristics of a system based on fuzzy inference rules. In this paper, a T-S fuzzy system is used to detect the divergence of EKF and adapt filter. Takagi and Sugeno propose a fuzzy modeling approach for model nonlinear

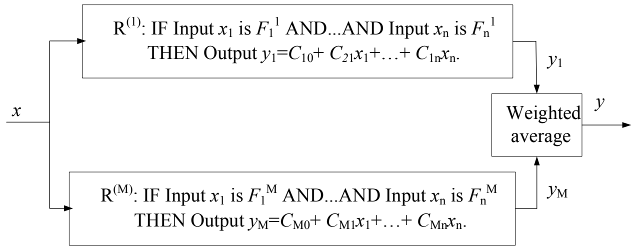

Fig. 4. T-S fuzzy system

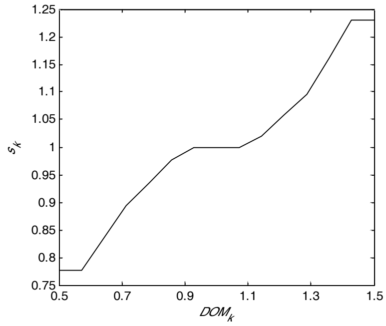

Fig. 5. Output surface of FIS

systems, and the T-S fuzzy system represents the conclusion by functions. The typical T-S system is shown in Fig. 4.

A typical rule in the T-S model has the form: IF Input x_1 is F_1^1 and Input x_2 is F_2^1…and Input x_n is F_n^1 THEN Output

$$y_k=f_k(x_1, x_2…x_n)=C_{k0}+ C_{k1}x_1+…+ C_{kn}x_n.$$

where C_{ki} (i=0~n) are constants in the kth rule. For the first-order model, it has the rule in the form: IF Input x_1 is F_1^1 and Input x_2 is F_2^1 THEN Output

$$y_k=C_{10}+ C_{11}x_1+ C_{12}x_2.$$

where F_1^1 and F_2^1 are fuzzy sets and C_{10}, C_{11} and C_{12} are constants.

For a zero-order model, the output level is a constant: IF Input x_1 is F_1^1 and Input x_2 is F_2^1 THEN Output $y_k=C_{10}$.

The output is the weighted average of the y_k.

$$y=\sum_{k=1}^{M}\lambda_k \cdot y_k \tag{30}$$

where the weights ω_k are computed as

$$\lambda_k=\frac{\prod_{i=1}^{n}\mu_{F_i^k}(x_1)}{\sum_{j=1}^{M}[\prod_{i=1}^{n}\mu_{F_i^k}(x_1)]} \tag{31}$$

where $\sum_{j=1}^{M}\lambda_i=1$, and μ represents the membership.

Fig. 5 shows the output of defuzzification. When the input value of DOM_k is around one, it reveals that the actual value of the innovation covariance is close to its theoretical value, and the output value of fuzzy factor s_k is around one.

3.2 Real-time adaptive extended kalman filter

Due to the fuzzy reasoning (fuzzy inference), the fuzzy defuzzification and the calculation of fuzzification, it is the essential to make a tradeoff between the accuracy and the computational burden for AEKF. Therefore, a real-time adaptive extended Kalman filter (RAEKF) based on exponential function is proposed in this paper to reduce the computational burden and improve the real-time performance simultaneously.

According to Fig. 5, it can be seen that the part waveform of the FIS output and the waveform of constant voltage power supply charging for the capacitor are similar. The formula of charging is designed as

$$y(t) = K_p(1 - \exp(-t / \tau)) \tag{32}$$

where K_p is the final value of response, t is time, and τ *is* the time constant. According to Fig. 5, the output equation of fuzzy controller can be expressed approximately as
when $0.5 \le DOM_k < 1$, then

$$\begin{aligned} s_k &= 0.11[1 - \exp(-|DOM_k - 0.75| / 0.05)] \\ &\times sig(DOM_k - 0.75) + 0.89 \end{aligned} \tag{33}$$

when $1 \le DOM_k < 1.5$,then

$$\begin{aligned} s_k &= 0.11[1 - \exp(-|DOM_k - 1.25| / 0.05)] \\ &\times sig(DOM_k - 1.25) + 1.11 \end{aligned} \tag{34}$$

where $sig(\cdot)$ is the sign function. The curve of the above simple exponential function is shown in Fig. 6.

Comparing Fig. 5 with Fig. 6, the two graphics are approximate. Therefore, an exponential function instead of fuzzy controller is used to obtain the real-time adaptive adjustment factor s_k.

In RAEKF, the exponential function is prescribed generally as

$$s_k = A_p[1 - \exp(-|DOM_k - x| / \tau)]sig(DOM_k - x) + y \tag{35}$$

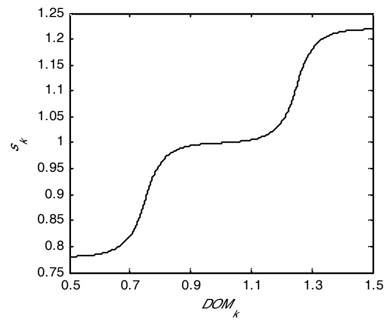

Fig. 6 The curve of adjustment factor s_k

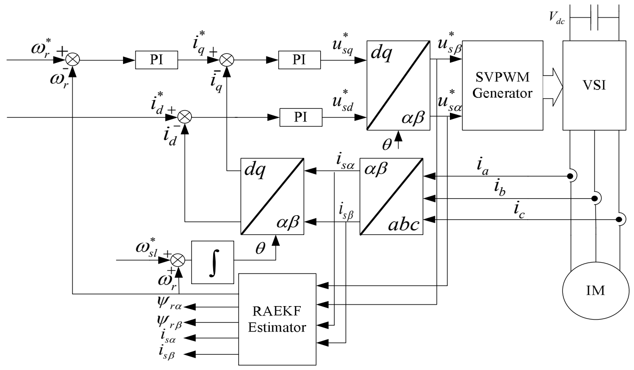

Fig. 7. System block frame of sensorless vector control based on RAEKF

where A_p and τ can change the performance of the filter. A is one-fifth of s_k maximum amplitude. τ is set to change curvature of the curve. x and y are the horizontal and vertical curve offset value, respectively.

The structure of sensorless vector control system for induction motors is shown in Fig. 7. The system adopts double loop control structure, and they are speed and current controller, respectively. The voltage and the phase current of the induction motor are transformed to α-β reference frame, which are the inputs of RAEKF. The rotor speed is estimated, which is the input of speed controller. The control voltage ($u_{s\alpha}$*, $u_{s\beta}$*) are transformed to u_{sd}* and u_{sq}*, which are the outputs of current controller. Finally, a induction motor is regulated by a PWM inverter which are controlled by the outputs of SVPWM.

4. Experimental Results

The proposed method is implemented to validate the performance of the estimator on experimental platform based on TMS320F28335, and the clock frequency of TMS320F28335 is 150 MHz. Table 1 shows the parameters of the induction motor in the experiment, and Fig. 8 shows the experimental system. The induction motor is driven by the two level voltage inverter. The switching frequency of the inverter is 8 kHz, the execution time of traditional EKF is 50 μs, the execution time of AEKF is 75 μs, and the execution time of RAEKF is 60 μs. The initialization parameters for EKF and RAEKF are as follows:

$$R = diag[0.1, 0.1],$$
$$Q = diag[2\times10^{-2}, 2\times10^{-2}, 2\times10^{-3}, 2\times10^{-3}, 1] .$$

Table 1. Motor parameters

P_N	1.1 kW	R_s	5.27 Ω
U_N	380 V	R_r	5.07 Ω
I_N	2.7 A	L_m	0.421 H
F_n	50 Hz	L_s	0.423 H
T_L	7.5 N· m	L_r	0.479 H
J	0.02 kg· m^2	σL_s	0.053 H
n_N	1410 r/min	P	2

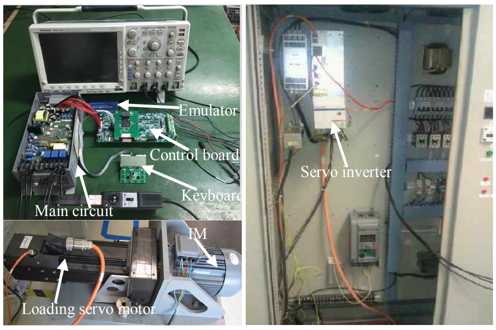

Fig. 8. Experimental platform

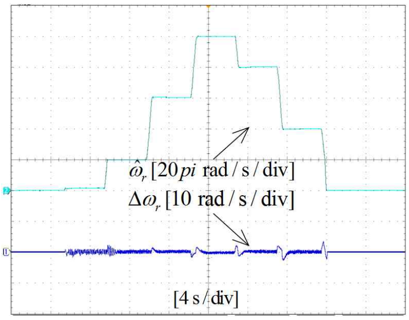

Fig. 9. Experimental results based on RAEKF in wide speed range

4.1 Experimental verification for speed estimation during full speed and low speed

Fig. 9 shows the response based on RAEKF when the given speed changes six steps, and the whole range of operating speed is contained. At the beginning, the motor operates at 2*pi* rad/s. Then, the motor accelerates to 20*pi* rad/s, 60*pi* rad/s and 100*pi* rad/s, respectively. Last, the motor decelerates to 80*pi* rad/s and 40*pi* rad/s, respectively. As presented in Fig. 9, the estimated speed can be is coincided with the actual speed, and it indicates that the tracking performance of RAEKF is good.

Fig. 10 shows the experimental result when the motor operates forward to reversal at low speed. At the beginning, the motor is operating at +100*pi* rad/s. Then, the motor decelerates to zero and accelerates to -100*pi* rad/s. From the experimental result, it shows that the current has no oscillation and transition during the motor speed reversal. In addition, the estimated speed based on RAEKF also tracks on the actual speed well, and the motor can switch smoothly at zero-crossing position.

In order to make further performance verification of the proposed method, a loading experiment is implemented at 1*pi* rad/s. Fig. 11 presents the experimental results based on RAEKF at 1*pi* rad/s when a step load with 150% rated torque is added. At the beginning, the motor is operating at +1*pi* rad/s with no load. Then, a step load is added to the motor. It shows that the speed sensorless vector control system based on RAEKF has good loading ability. However, the fluctuation of motor speed and speed

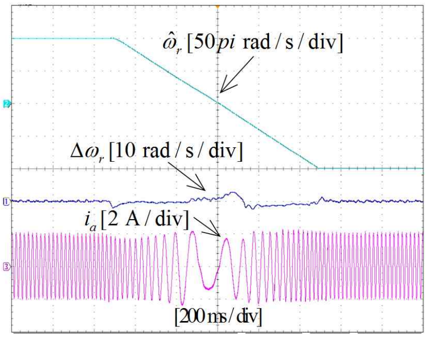

Fig. 10. Speed response and stator current based on RAEKF when the given speed ranges from +100*pi* rad/s to -100*pi* rad/s

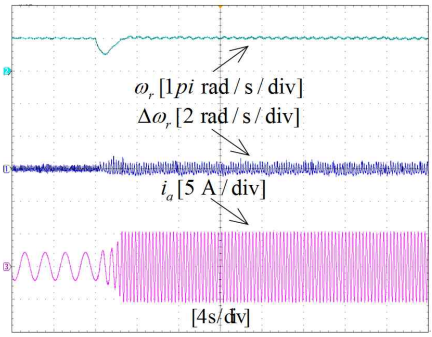

Fig. 11. Experimental results based on RAEKF at 1*pi* rad/s with step load from 0 to 150% rated torque

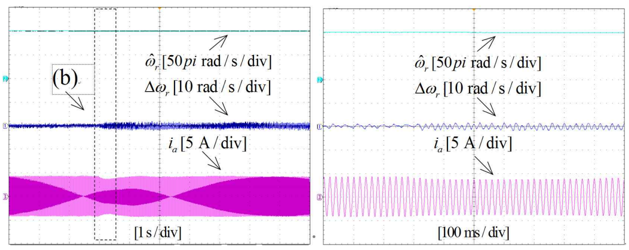

(a) (b)

Fig. 12. Speed estimation performance based on RAEKF when speed-sensor fails at 100*pi* rad/s with 100% rated torque

estimation error become larger. But the motor can operate stably and well at low speed with load, and the current waveform is not distorted and remains sine.

Fig. 12 shows that the speed estimation performance based on RAEKF when speed-sensor fails at 100*pi* rad/s with 100% rated torque. The speed based on speed-sensor is used feedback speed before 4 s, and the speed based on RAEKF is used feedback speed after 3 s to simulate encoder failure. From the experimental results, the current waveform has slight oscillation, but it restores stability quickly and the motor can operate stably. Therefore, RAEKF is particularly suitable for the products of the speed-sensorless compact drives composing of a motor and an inverter, the applications such as electrical or hybrid vehicles where both a resolver as speed sensor and a speed estimation algorithm which are used and required for safety purposes in case the speed-sensor fails.

Figs. 9-12 demonstrate the correctness of the speed estimation system based on RAEKF.

4.2 Robustness to motor parameter variations

In order to validate the robustness of RAEKF with motor parameter variations, the experiments are implemented with parameter mismatch in this paper, and the given speed is 2*pi* rad/s with no load. Fig. 13 shows experimental results using EKF and RAEKF with the stator resistance deviation $|\Delta R_s|$=30%. As presented in Fig. 13, the fluctuation of estimated speed based on EKF is larger than RAEKF when R_s mismatches. In addition, the speed estimation error is 2.2 rad/s using EKF. However, the speed estimation error is 1.2 rad/s based on RAEKF, which is smaller than EKF with mismatched R_s.

Fig. 14 presents the experimental results of EKF and RAEKF at 2*pi* rad/s with the rotor resistance deviation $|\Delta R_r|$=30%. It can be seen that the estimated speed based on EKF has a larger fluctuation when R_r mismatches, and the speed estimation error is 2.1 rad/s. However, the speed estimation error using RAEKF is only 1.1 rad/s, and the speed estimation fluctuation and error of RAEKF are smaller, compared with EKF.

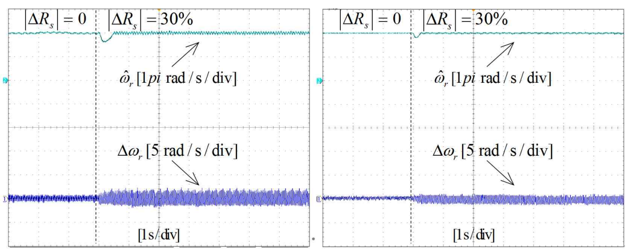

(a) (b)

Fig. 13. Experimental comparison of the estimated speed and the speed estimation error at 2*pi* rad/s with the stator resistance deviation $|\Delta R_s|$=30%. (a) EKF. (b) RAEKF.

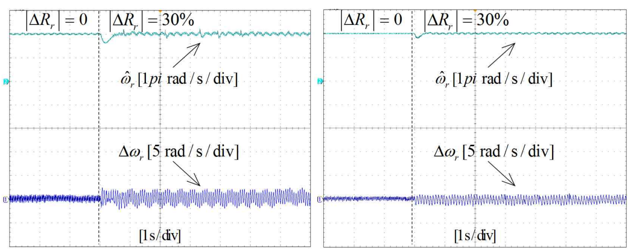

(a) (b)

Fig. 14. Experimental comparison of the estimated speed and the speed estimation error at 2*pi* rad/s with the rotor resistance deviation $|\Delta R_r|$=30%. (a) EKF. (b) RAEKF.

Fig. 15 presents the experimental results of EKF and RAEKF at 2*pi* rad/s with the mutual inductance deviation $|\Delta L_m|$=30%. It can be seen that the estimated speed based on EKF has a larger fluctuation when L_m mismatches, and the speed estimation error is 2.0 rad/s. However, the speed estimation error based on RAEKF is only 1.0 rad/s, and the speed estimation fluctuation and error of RAEKF are smaller, compared with EKF.

Fig. 13, Fig. 14 and Fig. 15 confirm that EKF is more sensitive to the motor parameter variations, and the robustness of RAEKF to motor parameter variations is better than EKF. The reason is that the noise matrix is fixed in EKF, and the modeling error cannot be tracked real-time when motor parameter variations. However, the adaptive adjustment factors are introduced in RAEKF, and the influence of modeling error can be weakened real-time by tuning adjustment factor in real-time.

4.3 With gross external disturbance

Fig. 16 presents the experimental results based on EKF and RAEKF when a external disturbance occurs at 100*pi* rad/s. In the experimental, a pulse that valued 2A is added to current detection channel for simulating external disturbance occurs. From the experimental results, both EKF and RAEKF are affected by external disturbance, but the estimated speed fluctuation and speed estimation error based on EKF is larger than RAEKF. The estimated speed

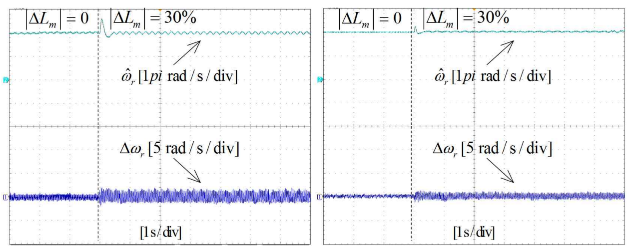

(a) (b)

Fig. 15. Experimental comparison of the estimated speed and the speed estimation error at 2*pi* rad/s with the mutual inductance deviation $|\Delta L_m|$=30%. (a) EKF. (b) RAEKF

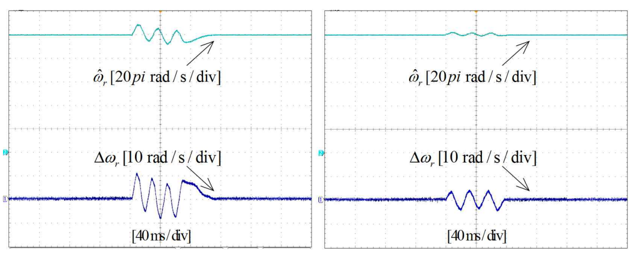

(a) (b)

Fig. 16. Experimental comparison of the estimated speed and the speed estimation error at 100*pi* rad/s with gross external disturbance. (a) EKF. (b) RAEKF

fluctuation based on EKF is 30 rad/s, and the speed estimation error is 11 rad/s when a disturbance occurs. However, The estimated speed fluctuation based on RAEKF reduces to 6 rad/s, and the speed estimation error reduces to 5 rad/s. Therefore, the influence of external disturbance to system can is weakened effectively, and the anti-error ability of system is improved obviously by RAEKF.

4.4 With gross estimation error

Fig. 17 presents the experimental results based on EKF and RAEKF at 100*pi* rad/s when a gross estimation error occurs. In the experimental, a pulse which valued 1 is added to $\tilde{\psi}_{r\alpha}$ for simulating internal estimation error occurs. From the experimental results, both EKF and RAEKF are affected by internal estimation error, but the estimated speed fluctuation and speed estimation error based on EKF is larger than RAEKF. The estimated speed fluctuation based on EKF is 28 rad/s, and the speed estimation error is 12 rad/s when a gross estimation error occurs. However, The estimated speed fluctuation based on RAEKF reduces to 8 rad/s, and the speed estimation error reduces to 4 rad/s. Therefore, RAEKF has better anti-estimation-error performance, compared with EKF.

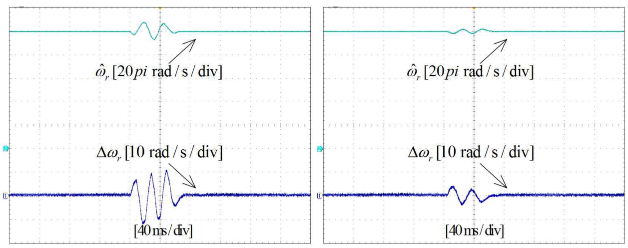

(a) (b)

Fig. 17. Experimental comparison of the estimated speed and the speed estimation error at 100*pi* rad/s with gross estimation error. (a) EKF. (b) RAEKF

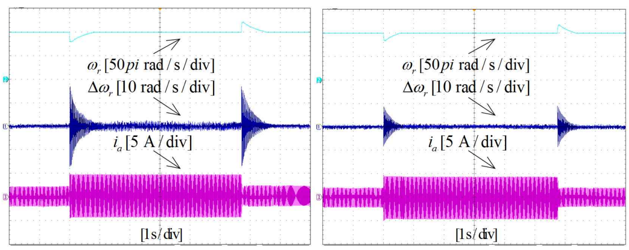

(a) (b)

Fig. 18. Experimental results based on EKF and RAEKF at 100*pi* rad/s when a step load is added with 100% rated torque. (a) EKF. (b) RAEKF

Table 2. Comparison of the speed estimation error

Algorithm	With gross external disturbance	With gross estimation error	With $\lvert\Delta R_s\rvert$=30%	With $\lvert\Delta R_r\rvert$=30%	With $\lvert\Delta R_m\rvert$=30%
IMM-EKF	7rad/s	8 rad/s	1.5 rad/s	1.6 rad/s	1.3 rad/s
RAEKF	5 rad/s	4 rad/s	1.2 rad/s	1.1 rad/s	1.0 rad/s

4.5 Dynamic performance verification with step load

Fig. 18 compares the experimental results with EKF and RAEKF when a step load is added with 100% rated torque. At the beginning, the motor operates at 100*pi* rad/s with no load, then a step load is added to the motor, and runs for some time with load. Last, the load is removed from the motor. It can be seen that both EKF and RAEKF can operate stably with load. However, the maximum error of the speed estimation based on RAEKF is smaller than EKF, and it reduces to 9 rad/s from 18 rad/s during the loading and deloading. In addition, the speed estimation error using RAEKF is also smaller than EKF operates with load. Therefore, RAEKF is more effective to achieve the speed-sensorless control, and the dynamic tracking and steady performance are better with step load, compared with EKF.

5. Conclusion

In this paper, an adaptive speed estimation method based on RAEKF for induction motors has been proposed. The correctness and the effectiveness of the proposed method have been verified based on a sensorless IM drive. The experimental results demonstrate that RAEKF can effectively improve the model adaptability to the actual systems and the environmental variations. The maximum error of the speed estimation with disturbance and motor parameter mismatches is obviously reduced, and both the steady and transient performance is improved by using the proposed adaptive speed estimation method. Compared with the method of reference [19], the execution time of IMM-EKF is 155 µs, however, the execution time of the proposed RAEKF is only 60 µs. Table 2 shows the comparison of the speed estimation error with some specific conditions based on the two methods. From Table 2, it can be seen that the performance of the proposed RAEKF is better than IMM-EKF.

Nomenclature

α, β	Stationary reference frame axes.
d, q	Rotary reference frame axes.
a, b, c	Three-phase reference frame axes.
$i_{s\alpha}$, $i_{s\beta}$	α-Axis and β-Axis stator currents, A.
i_{sd}, i_{sq}	d-Axis and q-Axis stator currents, A.
i_a, i_b, i_c	a-Axis, b-Axis and c-Axis stator currents, A.
$u_{s\alpha}$, $u_{s\beta}$	α-Axis and β-Axis stator voltages, V.
u_{sd}, u_{sq}	d-Axis and q-Axis stator voltages, V.

$\psi_{r\alpha}$, $\psi_{r\beta}$ α-Axis and β-Axis rotor flux linkages, Wb.
V_{dc} DC link voltage, V.
$\square^*$ Reference quantity.
J Moment of inertia.
θ Rotor position.
ω_{sl} Slip frequency, rad/s.
ω_r Angular rotor speed, rad/s.
L_m Mutual inductance, H.
$L_{s\sigma}$ Stator leakage inductance, H.
$L_{r\sigma}$ Rotor leakage inductance, H.
L_s, L_r Stator and rotor inductances, H.
σ (=1-(L_m^2/L_sL_r)) Total leakage coefficient.
σ_r Rotor leakage coefficient.
σ_s Stator leakage coefficient.
R_s, R_r Stator and rotor resistances, Ω.
T_r (=L_r/R_r) Rotor time constant.
T Sampling period, μs.
v_k System noise.
w_k Measurement noise.
T_L Rated torque, N·m.
P Pole pair.
P_N Rated power, kW.
U_N Rated voltage, V.
I_N Rated current, A.
f_N Rated frequency, Hz
$\hat{\omega}_r$ Estimated speed, rad/s.
$\Delta\hat{\omega}_r$ ($=\omega_r-\hat{\omega}_r$) Speed estimation error, rad/s.
$\tilde{\bullet}$ Prediction value.
$\hat{\bullet}$ Update value.

References

[1] X. Sun, L. Chen, Z. Yang, and H. Zhu, "Speed-sensorless vector control of a bearingless induction motor with artificial neural network inverse speed observer," *IEEE Trans. on Mechatron.*, vol. 18, no. 4, pp. 1357-1366, Aug. 2013.

[2] T. Orlowska-Kowalska and M. Dybkowski, "A new formulation of reactive-power-based model reference adaptive system for sensorless induction motor drive," *IEEE Trans. Ind. Electron.*, vol. 62, no. 11, pp. 6797-6807, Nov. 2015.

[3] A. Accetta, M. Cirrincione, M. Pucci, and G. Vitale, "Closed-loop MRAS speed observer for linear inductionmotor drives," *IEEE Trans. Ind. Appl.*, vol. 51, no. 3, pp. 2279-2290, May/Jun. 2015.

[4] L. Zhao, J. Huang, N. Li, and W. Kong, "Second-order sliding-mode observer with online parameter identification for sensorless induction motodrives," *IEEE Trans. Ind. Electron.*, vol. 61, no. 10, pp. 5280-5289, Oct. 2014.

[5] R. Vieira, C. Gastaldini, R. Azzolin, and H. A. Gründling, "Sensorless sliding-mode rotor speed observer of induction machines based on magnetizing current estimation," *IEEE Trans. Ind. Electron.*, vol. 61, no. 9, pp. 4573-4582, Sep. 2014.

[6] S. Po-ngam and S. Sangwongwanich, "Stability and dynamic performance improvement of adaptive full-order observers for sensorless PMSM drive," *IEEE Trans. Power Electron.*, vol. 27, no. 2, pp. 588-600, Feb. 2012.

[7] M. Zaky, "Stability analysis of speed and stator resistance estimators for sensorless induction motor drives," *IEEE Trans. Ind. Electron.*, vol. 59, no. 2, pp. 858-870, Feb. 2012.

[8] W. Sun, Y. Yu, G. Wang, B. Li, and D. Xu "Design method of adaptive full order observer with or without estimated flux error in speed estimation algorithm," *IEEE Trans. Power. Electron.*, vol. 31, no. 3, pp. 2609-2626, Mar. 2016.

[9] C. Caruana, G. M. Asher, and M. Sumner, "Performance of HF signal injection techniques for zero-low-frequency vector control of induction machines under sensorless conditions," *IEEE Trans. Ind. Electron.*, vol. 53, no. 1, pp. 225-238, Feb. 2006.

[10] L. Xu, E. Inoa, Y. Liu, and B. Guan, "A new high-frequency injection method for sensorless control of doubly fed induction machines," *IEEE Trans. Ind. Appl.*, vol. 48, no. 5, pp. 1556-1564, Sep/Oct. 2012.

[11] F. Alonge, T. Cangemi, F. D'Ippolito, A. Fagiolini and A. Sferlazza, "Convergence analysis of an extended Kalman filter for sensorless control of induction motors," *IEEE Trans. Ind. Electron.*, vol. 62, no. 4, pp. 2341-2352, Apr. 2015.

[12] I. Alsofyani and N. Idris, "Simple flux regulation for improving state estimation at very low and zero speed of a speed sensorless direct torque control of an induction motor," *IEEE Trans. Power. Electron.*, vol. 31, no. 4, pp. 3027-3035, Apr. 2016.

[13] M. Habibullah and D. Lu, "A speed-sensorless FS-PTC of induction motors using extended Kalman filters," *IEEE Trans. Ind. Electron.*, vol. 62, no. 11, pp. 6765-6778, Nov. 2015.

[14] Y. Shi, K. Sun, L. Huang, and Y. Li, "Online identification of permanent magnet fluxbased on extended Kalman filter for IPMSM drive with position sensorless control," *IEEE Trans. Ind. Electron.*, vol. 59, no. 11, pp. 4169-4178, Nov. 2012.

[15] L. Idkhajine, E. Monmasson, and A. Maalouf, "Fully FPGA-based sensorless control for synchronous AC drive using an extended Kalman filter," *IEEE Trans. Ind. Electron.*, vol. 59, no. 10, pp. 3908-3918, Oct. 2012.

[16] N. K. Quang, N. T. Hieu, and Q. P. Ha, "FPGA-based sensorless PMSM speed control using reduced-order extended Kalman filters," *IEEE Trans. Ind. Electron.*, vol. 61, no. 2, pp. 6574-6582, Dec. 2014.

[17] Z. Yin, C. Zhao, J. Liu, and Y. Zhong, "Research on anti-error performance of speed and flux estimator for induction motor using robust reduced-order EKF," *IEEE Trans. Ind. Informatics.*, vol. 9, no. 2,

pp. 1037-1046, May. 2013.

[18] M. Barut, R. Demir, E. Zerdali, and R. Inan, "Real-time implementation of bi input-extended Kalman filter-based estimator for speed-sensorless control of induction motors," *IEEE Trans. Ind. Electron.*, vol. 59, no. 11, pp. 4197-4206, Nov. 2012.

[19] Z. Yin, C. Zhao, Y. Zhong, and J. Liu, "Research on robust performance of speed-sensorless vector control for the induction motor using an interfacing multiple-model extended kalman filter," *IEEE Trans. Power. Electron.*, vol. 29, no. 6, pp. 3011-3019, Jun. 2014.

[20] Z. Yin, G. Li, C. Du, J. Liu, X. Sun, and Y. Zhong, "An adaptive speed estimation method based on strong tracking extended Kalman filter with least-square for induction motors," *Journal of Power Electron.*, vol. 17, no. 1, pp. 149-160, Jan. 2017.

[21] K. Szabat, T. Orlowska-Kowalska, and M. Dybkowski, "Indirect adaptive control of induction motor drive system with an elastic coupling," *IEEE Trans. Ind. Electron.*, vol. 56, no. 10, pp. 4038-4042, Oct. 2009.

[22] M. Hilairet, F. Auger, and E. Berthelot, "Speed and rotor flux estimation of induction machines using a two-stage extended Kalman filter," *Automatica*, vol. 45, no. 8, pp. 1819-1827, Aug. 2009.

[23] V. Smidl and Z. Peroutka, "Advantages of square-root extended Kalman filter for sensorless control of AC drives," *IEEE Trans. Ind. Electron.*, vol. 59, no. 11, pp. 4189-4196, Nov. 2012.

[24] N. Salvatore, A. Caponio, F. Neri, S. Stasi, and G. L. Cascella, "Optimization of delayed-state kalman-filter-based optimization of delayed-state Kalman-filter-based control of induction motors," *IEEE Trans. Ind. Electron.*, vol. 57, no. 1, pp. 385-394, Jan. 2010.

[25] T. Schuhmann and W. Hofmann, "Improving operational performance of active magnetic bearings using Kalman filter and state feedback control," *IEEE Trans. Ind. Electron.*, vol. 59, no. 2, pp. 821-829, Feb. 2012.

[26] G. Foo, X. Zhang, and D. Vilathgamuwa, "A sensor fault detection and isolation method in interior permanent-magnet synchronous motor drives based on an extended Kalman filter," *IEEE Trans. Ind. Electron.*, vol. 60, no. 8, pp. 3485-3495, Aug. 2013.

Yanqing Zhang was born in Shaanxi, China, in 1989. He received the B.S. and M.S. degrees in Electrical Engineering from Xi'an University of Technology, Xi'an, China, in 2012 and 2015 respectively. He is currently a Ph.D. student in Electrical Engineering, Xi'an University of Technology. His main field of interest is high-performance control of ac motor.

Zhonggang Yin was born in Shandong, China, in 1982. He received the B.S., M.S. and Ph.D. degrees in electrical engineering from Xi'an University of Technology, Shaanxi, China, in 2003, 2006 and 2009, respectively. In 2009, he joined electrical engineering department of Xi'an University of Technology, where he is currently a professor. His research interests include high-performance control of ac motor, and digital control of power converters.

Guoyin Li was born in Chongqing, China, in 1992. He received the B.S. and M.S. degrees in electrical engineering from Xi'an University of Technology, Xi'an, China, in 2014 and 2017, respectively. Since 2017, he has been an Engineer with CRRC SRI Chongqing S&T Co.,Ltd. His research interests include high-performance control of ac motors and digital control of power converters.

Jing Liu was born in Anhui, China, in 1982. She received the B.S., M.S. and Ph.D. degrees in electronic engineering from Xi'an University of Technology, Shaanxi, China, in 2003, 2006 and 2009, respectively. In 2009, she joined electronic engineering department of Xi'an University of Technology, where she is currently an associate professor. Her research interests include the power semiconductor devices and their application to power electronic devices.

Xiangqian Tong was born in Shaanxi, China, in 1961. He received his B.S. degree in Electrical Engineering from Shaanxi Institute of Technology, Hanzhong, China, and the M.S. degree from Xi'an University of Technology, Xi'an, China, in 1983 and 1989, respectively, and the Ph.D. degree in Electrical Engineering from Xi'an Jiaotong University, Xi'an, in 2006. He joined the Xi'an University of Technology in 1989. Since 2002, he has been a Professor and the Academic Leader of Electrical Engineering with the Xi'an University of Technology. His current research interests include the application of power electronics in power system and control of power quality, especially the power filter, static synchronous compensator, and high voltage direct current.